An Experimental Study on Swirling Flow behind a Round Cylinder in the Horizontal Circular Tube

Tae-Hyun Chang*
Division of Mechanical and Automation Engineering, Kyungnam University,
449 Wolyoung Dong, Masan, Kyungnam 631-701, Korea
Hae Soo Lee
Department of Mechanical Engineering, Kyungnam University, Graduate School,
449 Wolyoung Dong, Masan, Kyungnam 631-701, Korea

An experimental study is performed for turbulent swirling flow behind a circular cylinder using 2-D PIV technique. The Reynolds number investigated are 10,000, 15,000, 20,000 and 25,000. The mean velocity vector, time mean axial velocity, turbulence intensity, kinetic energy and Reynolds shear stress behind the cylinder are measured before and behind the round cylinder along the test tube. A comparison is included with non swirl flow behind a circular and square cylinder. The recirculation zones are showed asymmetric profiles.

Key Words: Wake, PIV, Swirling Flow, Recirculating Region

1. Introduction

Wake, which has been a classical concern in flow analysis around a bluff body, must be studied in heat exchanger design. The effect of wake from an obstacle in the flow field separates flow, forms vortex yields aero dynamical drag, and structural vibration, and directly influences the turbulent mixing process. Coutanceau et al. (1959) compared the measured velocity for Reynolds numbers between 5 to 40 with calculated velocity in the wake behind a circular cylinder. Owen et al.(1980) analyzed the turbulent flow structure by using the average phase method. Cantwell (1975) and Coles (1983) explained the turbulent flow structure by using a flying hot wire and by measuring the average value of the Reynolds number terms in the turbulent momentum equation.

Boo Jung-sook (1985) analyzed the turbulent flow characteristics of a 2 dimensional wake behind a circular cylinder by a statistical method. Cho Ja-hee (1990) obtained average velocities, turbulent intensities, kinetic energy, and so on of the fluid in the wake behind a rectangular cylinder by a hot-wire anemometer. Kim et al.(1995) simultaneously measured and analyzed the velocity and temperature signal of the fluid behind a round tube ,while the heating of the cylinder was varied in the flow field, which had a temperature gradient. Choi et al.(1999) investigated the effect of wake flow characteristics and the vortex mechanism by using an external acoustic device. For a heat transfer-related investigation, Yoon et al.(1999) researched the effect of flow and heat transfer in gas turbine cascade by investigating the wake behind a rectangular cylinder.

The wakes of several kinds of cylinders have so far been researched by a hot wire anemometer, the LDV method, and a visualization method such as smoke and so. In these cases, the results consisted of no more than a point measurement at a point, and in case of using hot-wire anemometer, the results were not free from the prong interference.

* Corresponding Author,
E-mail : changtae@kyungnam.ac.kr
TEL : +82-55-249-2613; **FAX** : +82-55-249-2617
Division of Mechanical and Automation Engineering, Kyungnam University, 449 Wolyoung Dong, Masan, Kyungnam 631-701, Korea. (Manuscript **Received** April 6, 2005; **Revised** September 22, 2005)

Recently, Lee Hyun et al.(2001) investigated the flow characteristics in the wake behind a simple body by the Multivision PIV (Particle Image Velocimetry) method. Daichin et al.(2001) investigated the main flow velocity and turbulent intensity in the wake behind an elliptical structural body by the PIV method. To investigate of the wake behind a rectangular cylinder, Jang et al. (2001) obtained the average velocities of the flow in the wake by a numerical and the PIV method. Lee Man-bok et al.(2001) researched flow behavior near the wake behind a square cylinder by the PIV method. Chang et al.(2001) compared the wake between circular and rectangular cylinders. Doh (2001) researched the wake behind a round cylinder by the 3 dimensional PIV method.

However, most of these investigations were conducted for uniform cylinder entrance flow. But the entrance flow is almost a swirling flow, in the particular cases of a steam and hot water heater, a fan coil unit, and so on, which have a fan.

In this study, the average velocity, turbulent intensity, Reynolds stress, turbulent kinetic energy, and so on of the turbulent wake with swirl in the horizontal circular tube were investigated by using 2-D PIV. This research may simply and effectively contribute to heat exchanger design.

2. Experiment Apparatus

Figure 1 is a schematic diagram of the experimental apparatus used in this study. The test tube was manufactured by an acryl tube, which was of ∅90 mm in diameter, 3,000 mm in length, and 5 mm in thickness, and the round cylinder a ∅20 mm-diameter rod. The water tank of 300 mm × 600 mm × 200 mm, was installed outside of the test tube to reduce measurement error due to the refraction from the density difference of the fluid, when PIV system was used to measure the velocity profiles behind the round cylinder. Water was used as the working fluid, which can be sequen-

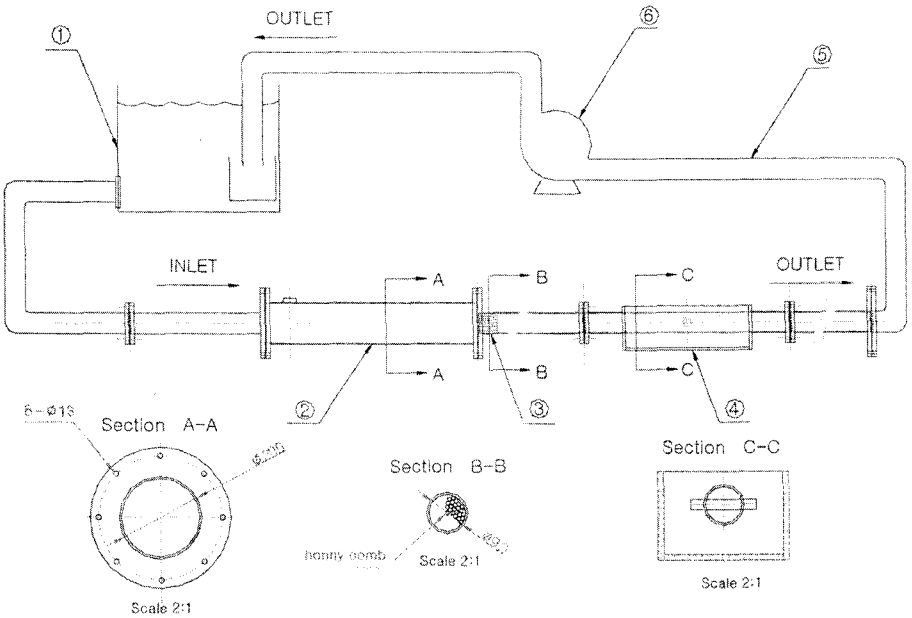

No	Apparatus	Material	No	Apparatus	Material
1	Water tank	Plastic	2	Swirl Chamber	Acrylic
3	Honny comb	Polypropylene	4	Test tube & Water Box	Acrylic
5	Flexible hose	Rubber	6	Water Pump (220V x 3.7kW)	Stainless Steel

Fig. 1 Schematic diagram of the experimental apparatus

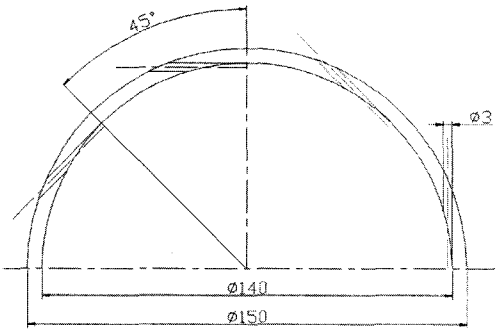

Fig. 2 Cross section view through the swirl generator

tially circulated through the swirl chamber, the swirl generator, the test tube, the circulating pump (220 V×3.75 kW), and the water tank. In order to adjust a Reynolds number in the test tube, a RPM controller of the pump was used. To produce a steady flow velocity without swirl, a honeycomb was installed at the entrance of the test tube.

A swirl generator was a ∅150-diameter acryl tube, which was tangentially drilled with ∅3 mm holes to the outer diameter of tube by 8 rows in 45° space. Fig. 2 indicates the cross section of the swirl generator.

2.1 Test method

An air-cooled Ar-ion laser, of 500 mW was used as the light source. To easily transport the light source, LLSP (Laser Light Sheet Probe), which could transport light through an optical cable, was used. Furthermore, the LLSP can control the thickness of laser layer to about 1 mm. The optical cable was 10 m in length. To generate a pulsating light source, AOM (Acoustic Optical Modulator) was used. A Panasonic CCD (Charge Couple Device) camera (WV3P310), which can produces images at 30 cuts per second, was used to obtain image of the flow field. To record the images, a digital recording method was used. To transport the images obtained in the gray level from 0 to 255 phases to the computer, a DT3155 (640×480 pixel) board was used. The particle used in the test was nylon 12 (80 μm). The working fluid was 80℃ distilled water, Fig. 3 shows the PIV system used in this test.

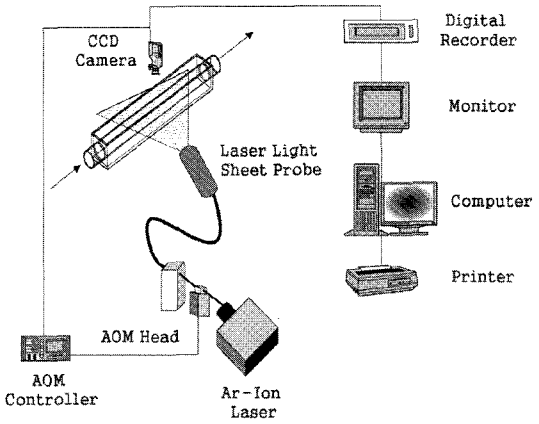

Fig. 3 Schematic arrangement of the PIV system

3. Result and Evaluation

3.1 Velocity vector

Figure 4 indicates instantaneous velocity vector with swirl at the entrance of the round cylinder when Re=20,000. The instantaneous velocity vector with swirl is a negative velocity vector at the center of the test tube and a positive velocity vector near the tube wall, a result that is the same as those of other investigations. Fig. 5 indicates a velocity vector without swirl when Re=10,000. A recirculation region is clearly shown.

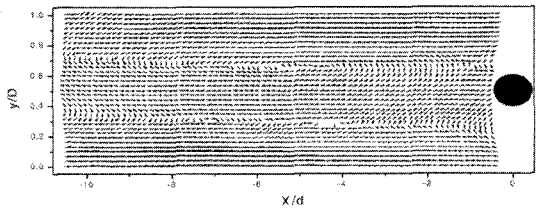

Fig. 4 Velocity vector profiles with swirl for Re=20,000 the entry of the round cylinder

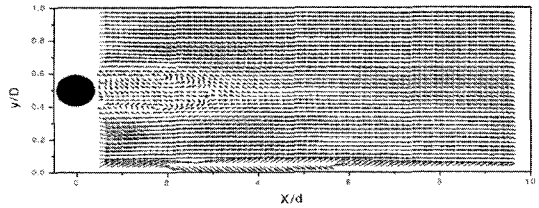

Fig. 5 Time-mean velocity vector profiles behind the round cylinder for Re=10,000

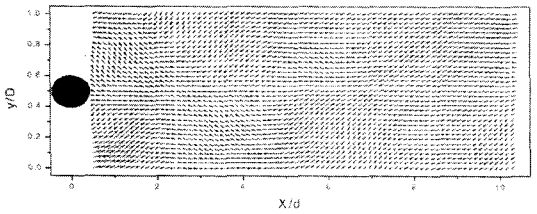

Fig. 6 Velocity vector profiles with swirl for Re=20,000 behind the round cylinder

Figure 6 indicates an instantaneous velocity vector with swirl behind the round cylinder when Re=20,000. The initial shear layer alternately separated from the both ends of the cylinder and formed a circular shape vortex, which tended to move downstream with a big curvature. This behavior is a big difference from the flow at the entrance of cylinder in Fig. 4.

3.2 Average velocity

Mizota et al.(1981) and Okajima et al.(1982) have measured the flow near the region behind a rectangular cylinder, where the flow was reversed by heating wire probes in a row. They stated that the variation of the flow was significantly related to the drag and lift force and Strouhal number. Cantwell (1975) announced that the re-circulating region was 1.1d when $Re=1.0\times10^5$ behind a round cylinder, and Owen et al.(1980) reported the region was about 1.3d when $Re=1.67\times10^5$ in a semispherical model.

Figure 7 shows the local axial velocity profile with swirl for Re=20,000 at the entrance of the round cylinder. This profiles, which was calculated from an instantaneous velocity vector in Fig. 4, shows the negative velocity of the flow at the tube center and the maximum positive velocity near the tube wall. These results coincided with previous results of swirl flow.

Figures 8~10 give the results of measured flow of the wake behind a round cylinder when Re=10,000, 30,000 and 50,000. The re-circulating region behind a round cylinder, which was 1.0d~1.5d, reduced, according to the Reynolds number increment. The maximum velocity profile appeared at y/D=0.2 or 0.8 near the test tube wall.

Figure 11 shows the result of the measured wake of a square cylinder without swirl when

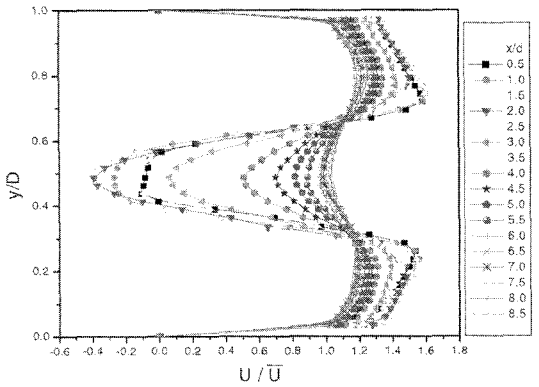

Fig. 8 Local axial velocity profiles without swirl for Re=10,000 behind the round cylinder

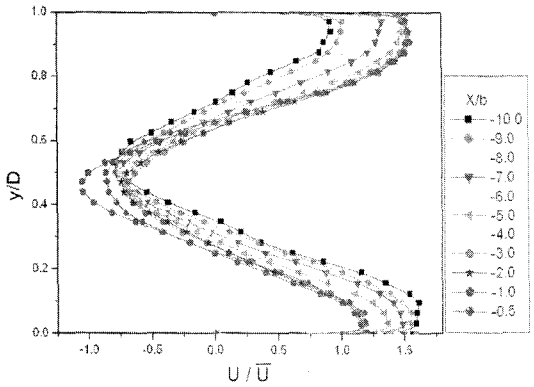

Fig. 7 Local axial velocity profiles with swirl for Re=20,000 at the entry of the round cylinder

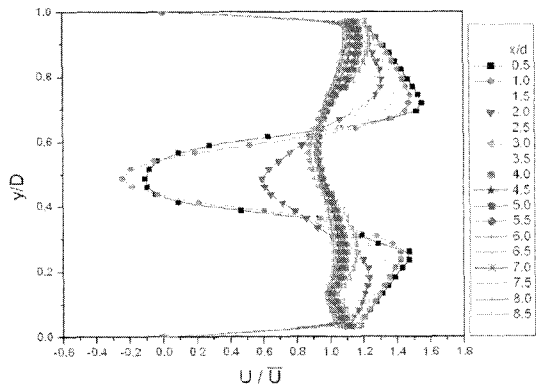

Fig. 9 Local axial velocity profiles without swirl behind the round cylinder for Re=30,000

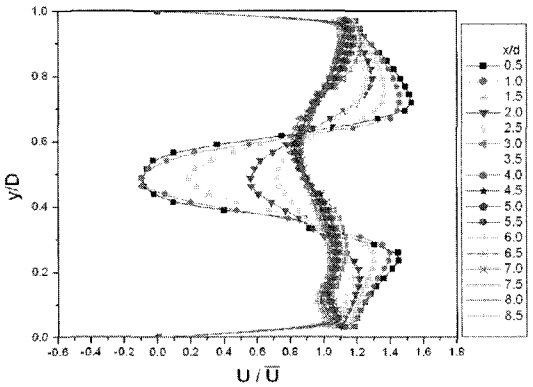

Fig. 10 Local axial velocity profiles without swirl behind the round cylinder for Re=50,000

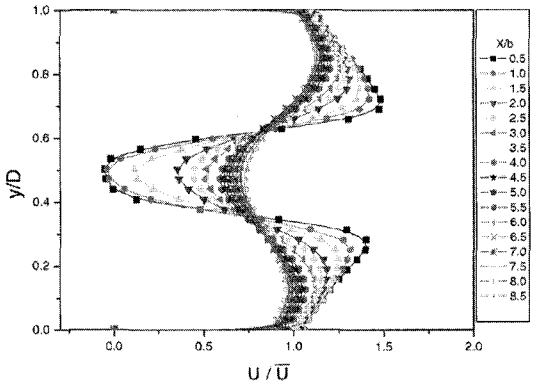

Fig. 11 Local Axial velocity profiles without swirl behind the square cylinder for Re=10,000

Re=10.000 and the re-circulating region is 1.0~1.5d. This results is in good agreement with the results of Cantwell (1975) and Owen et al. (1980).

Figures 12~15 shows the axial velocity profiles with the swirl behind a cylinder for Re=10,000, 15,000, 20,000 and 25,000. There is flow in the asymmetry region at X/d=0.5 that is different from the non swirl flow. When X/d is increased, this region is reduced by the decaying of swirl. Tangential velocity in swirl flow is thought to depends on the rotating direction of the flow. In Fig. 12 for Re=10.000, the re-circulating region is at X/d=0.5, is shorter than the result of Fig. 8 without swirl, and shows an asymmetric two cell. feature. As the swirl is decayed, this region is gradually reduced and shown as a maximum positive at the tube wall.

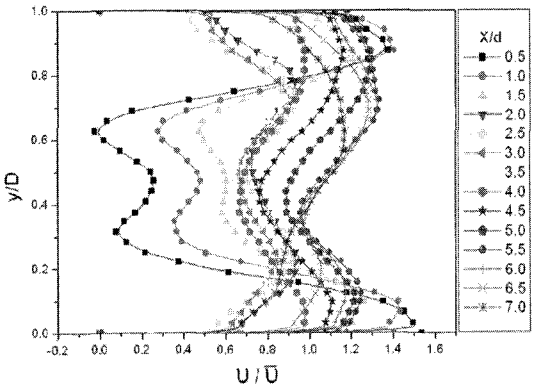

Fig. 12 Local axial velocity profiles with swirl for Re=10,000 behind the round cylinder

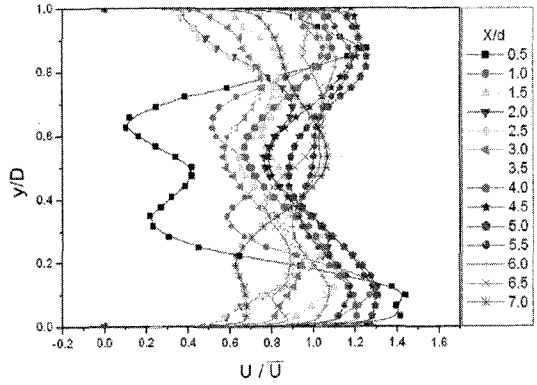

Fig. 13 Local axial velocity profiles with swirl for Re=15,000 behind the round cylinder

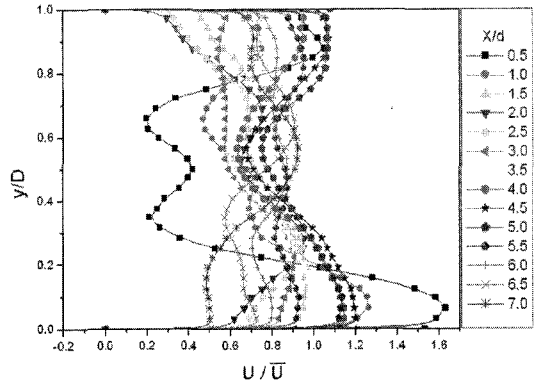

Fig. 14 Local axial velocity profiles with swirl for Re=20,000 behind the round cylinder

Regardless of the Reynolds number, the maximum asymmetric re-circulating region is placed

at X/d=0.5, and the maximum velocity profile is at both the test tube walls. This phenomenon in the swirl flow is thought due to the tangential velocity caused by the rotating direction of the flow. But as the swirl is decayed, this region is gradually reduced.

Figure 16 shows the comparison between the local axial velocity profiles at center line behind the round and square cylinders with swirl for Re=10,000, 15,000, 20,000 and 25,000 and without swirl for Re=10,000. $U/\overline{U}$ of the swirl flow is 0.2~0.86 higher than that of the non-swirl, and the $U/\overline{U}$ of the non-swirl flow is 0.0~−0.4 lower than that at the swirl flow.

But after X/d=0.3 as the swirl is decayed, $U/\overline{U}$ of the swirl flow shows that the flow has the same velocity profiles as the non-swirl flow does. This phenomenon is caused by the decay of the tangential velocity of the swirl flow.

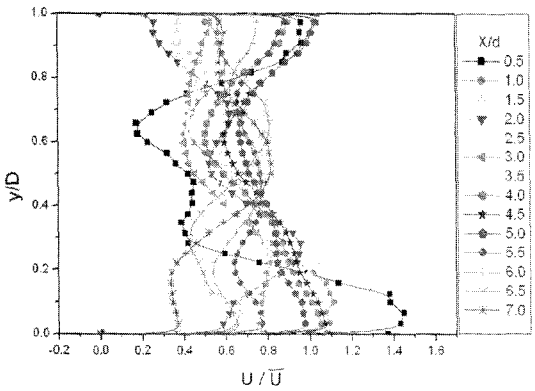

Fig. 15 Local axial velocity profiles with swirl for Re=25,000 behind the round cylinder

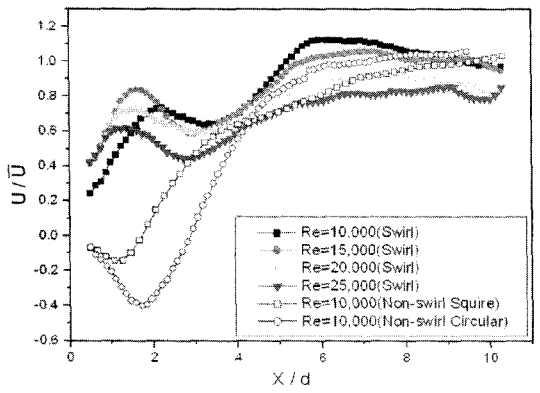

Fig. 16 Local axial velocity profiles with and without swirl at the center line behind the round and squire cylinder

3.3 Turbulent intensity

Figure 17 shows the contour of the turbulent axial intensity profiles without swirl behind the round cylinder for Re=30,000. Like previous studies what have two cell feature for these profiles, this study found as X/d is increased, the intensity is gradually decayed.

Figure 18 shows the contour of the axial turbulent intensity profiles with swirl for Re=20,000 at the entry of the round cylinder. This contour becomes the minimum value near tube wall and y/d=0.3 and X/d=−0.2~−9.0. This is regarded as the result of strong swirl for Re=20,000. But, in Fig. 19, an axial turbulent intensity profile with swirl for Re=20,000 behind the round cylinder is shown the minimum value at y/d=0.2~0.9 near the tube wall and the maximum value at X/d=0~1.0 and y/D=0, 1.0 near the tube wall. Meanwhile, the axial turbulent inten-

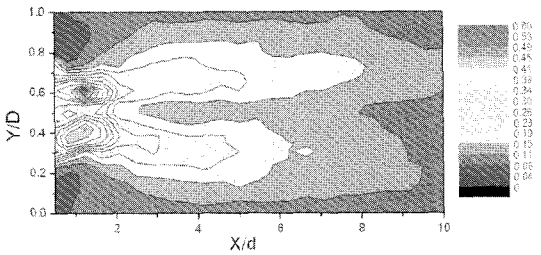

Fig. 17 Contour of turbulent axial intensity profiles without swirl behind the round cylinder for Re=30,000

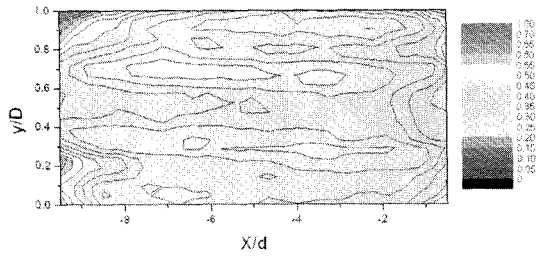

Fig. 18 Contour of axial turbulent intensity profiles with swirl for Re=20,000 at the entry of the round cylinder

sity profile behind a cylinder decreases along the test tube. This decrease is due to the tangential velocity component of the flow with the decaying of swirl.

Figure 20 shows the contour of the radial turbulent intensity profiles with swirl behind a cylinder. The profiles reach the minimum value at y/D=0.2~0.8 but the maximum near the test the tube wall. These profiles are balanced turbulent intensity profiles different from the axial turbulent intensity profiles. The swirl flow does not much affect the radial velocity component.

The local axial turbulent intensity profiles without swirl behind the round cylinder for Re= 30,000 are two cell as shown in Fig. 21. These profiles were calculated from the contour in Fig. 17 and they agreed with those of previous studies Kiya et al.(1985), and the Author.

The local axial turbulent intensity profiles without swirl behind the square cylinder for Re= 30,000 are bimodal are bimodal at X/b=0.5~ 1.0 but after this point, have a single peak, as shown in Fig. 22. This behavior means that the axial turbulent intensity behind the square cylinder decays more than that behind the round cylinder.

The local axial turbulent intensity profiles with swirl at the entry of the round cylinder for Re= 20,000 are shown in Fig. 23. These profiles were calculated from the contour of axial turbulent intensity profiles in Fig. 18. They are asymmetric different from those of the non-swirl flow. It is thought that these phenomena were caused by because of the tangential velocity of the swirl flow.

The local axial turbulent intensity profiles with swirl for behind the round cylinder are shown in Fig. 24. They are similar to those of the turbulent intensity and are asymmetric as in Fig. 23, but can

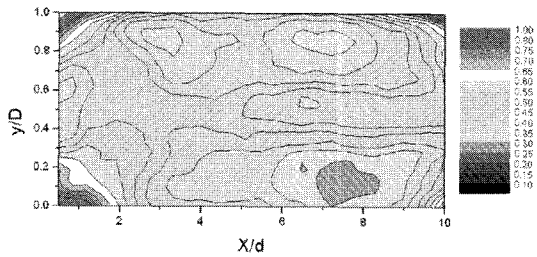

Fig. 19 Contour of axial turbulent intensity profiles with swirl for Re=20,000 behind the round cylinder

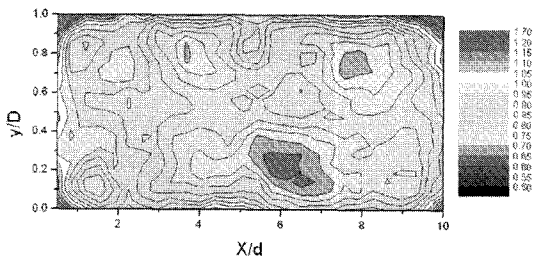

Fig. 20 Contour of radial turbulent intensity profiles with swirl for Re=20,000 behind the round cylinder

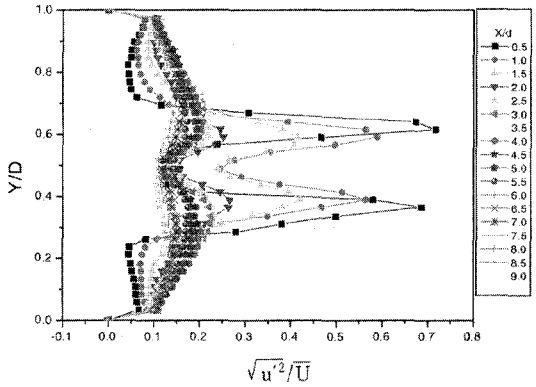

Fig. 21 Time-mean local axial turbulent intensity profiles without swirl behind the round cylinder for Re=30,000

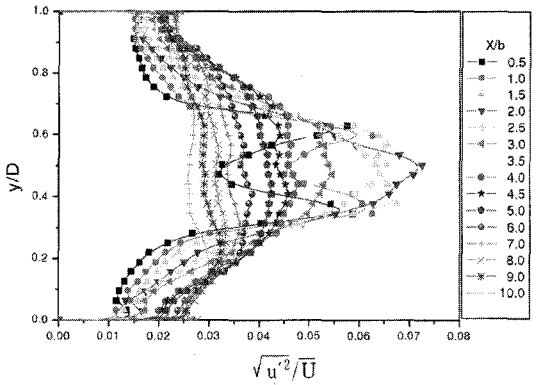

Fig. 22 Time-mean local axial turbulent intensity profiles behind the square cylinder for Re= 30,000

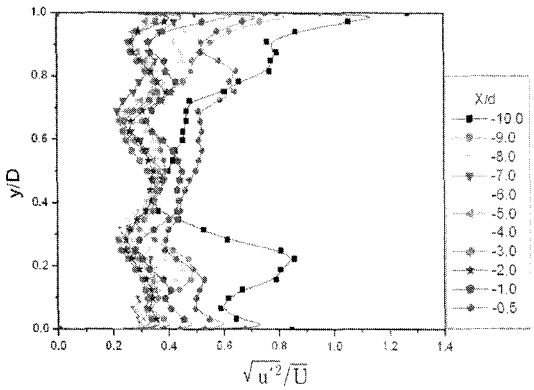

Fig. 23 Local axial turbulent intensity profile with swirl for Re=20,000 at the entry of the round cylinder

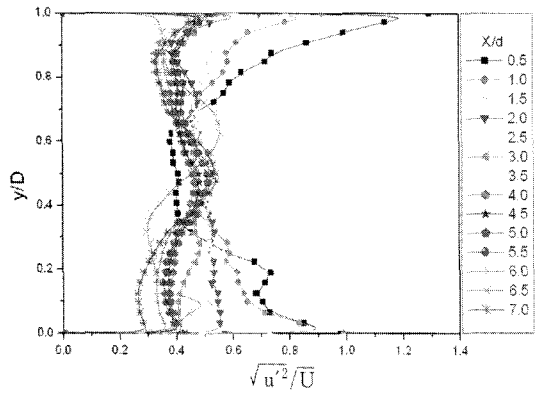

Fig. 24 Local axial turbulent intensity profile with swirl for Re=20,000 behind the round cylinder

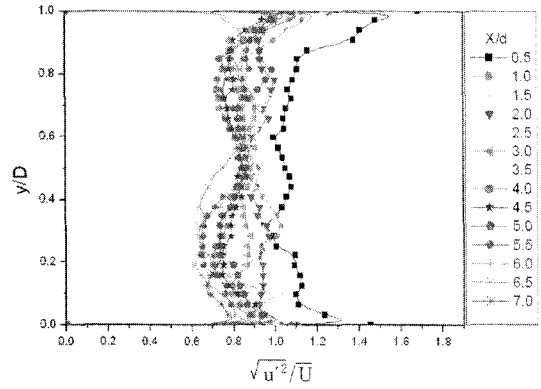

Fig. 25 Local radial turbulent intensity profile with swirl for Re=20,000 behind the round cylinder

become symmetric except at X/d=0.5. These results are presumed that as the swirl flow passes through a round cylinder, it is gradually decayed. The intensity approaches to $\sqrt{u'^2}/\bar{U}=0.4\sim0.5$ at the center of the wake.

The local radial turbulent intensity profiles with swirl for Re=20,000 behind the round cylinder are shown in Fig. 25. They are less asymmetric than the axial turbulent intensity and $\sqrt{u'^2}/\bar{U}=0.8\sim1.1$ at the center of tube, which is also higher than that of axial. The decay of the radial turbulent intensity of the wake with swirl is less than that of the axial turbulent intensity.

3.4 Turbulent shear stress and kinetic energy

Figure 26 shows the contour of the turbulent shear stress profiles without swirl behind a round cylinder for Re=30,000. The momentum changes actively near the region behind the round cylinder at X/d=2~6 and y/D=0.2~0.6.

Figure 27 shows the contour of the turbulent shear stress profiles with swirl behind the round

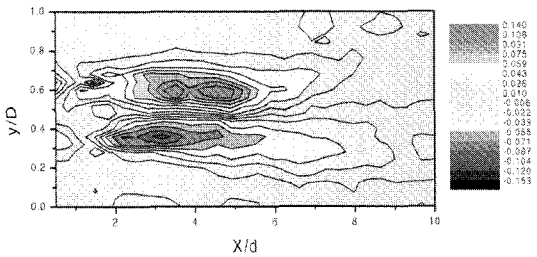

Fig. 26 Contour of Reynolds Shear Stress profiles without swirl behind the round cylinder for Re=30,000

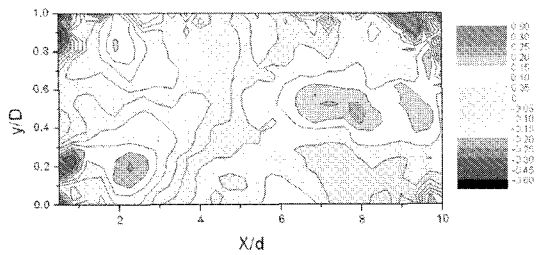

Fig. 27 Contour of Reynolds shear stress profiles τ_{xy} with swirl for Re=20,000 behind the round cylinder

cylinder. In particular, the shear stress is a negative minimum value near y/D=0.2, y/D=0.8~1.0 and X/d=0~2.5. This result implies that compared with the result of Fig. 26, it is a negative value in the near region behind the cylinder.

Figures 28 and 29 show the contour of the kinetic energy profiles with and without swirl behind the round cylinder. The kinetic energy without swirl is maximum at X/d=1.0~2.0 and y/D=0.4~0.6, and generally behaves similar to the axial turbulent intensity of the main flow. However, the contour of the kinetic energy profiles with swirl for Re=20,000 behind the round cylinder become the minimum value at y/D=0.2~0.8 and X/d=4~9.0 like the axial and radial turbulent intensities, and sinks downward. This phenomenon thought to be related to the decaying with swirl.

Figures 30 and 31 show the local Reynolds stress profiles without swirl behind the round and the square cylinder. It has maximum contradictory values near y/D=0.4~0.6 similar to previous results and has minimum at y/D=0.5, which is very similar to the result of Kiya et al.(1985).

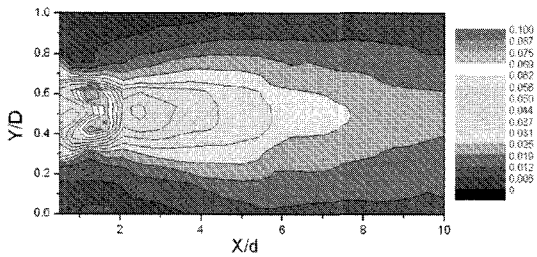

Fig. 28 Contour of kinetic energy profiles without swirl behind the round cylinder for Re=30,000

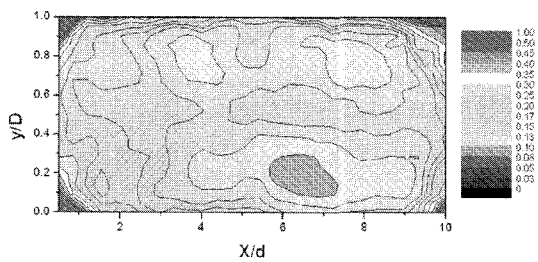

Fig. 29 Contour of kinetic energy profiles with swirl for Re=20,000 behind the round cylinder

Figure 32 is the local Reynolds shear stress profile with swirl for behind the round cylinder. The negative shear stresses and asymmetric phenomena appears at y/D=0, 0.2 and y/D=0.8~1.0, but as the swirl is decayed, it approaches to 0 after X/d=3.0 and y/D=0.3~0.6.

Figures 30 and 31 show entirely different profiles from the result of the non-swirl flow. As it were, the non-swirl flow behind the round or the square cylinder gave negative turbulent shear stress profiles along the centerline of the cylinder, but the stress of the swirl flow appeared as a negative, asymmetric feature near the perimeter of the cylinder.

Figure 33 shows the local kinetic energy profile

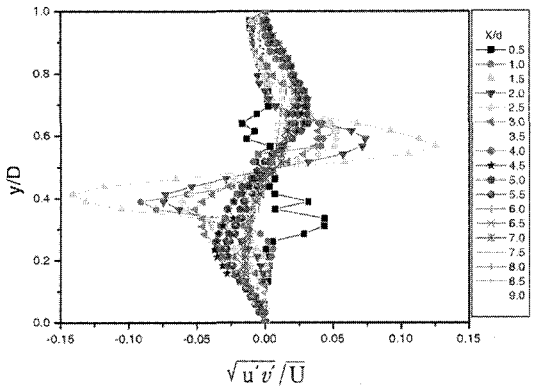

Fig. 30 Time-mean local Reynolds stress profiles without swirl behind the round cylinder for Re=30,000

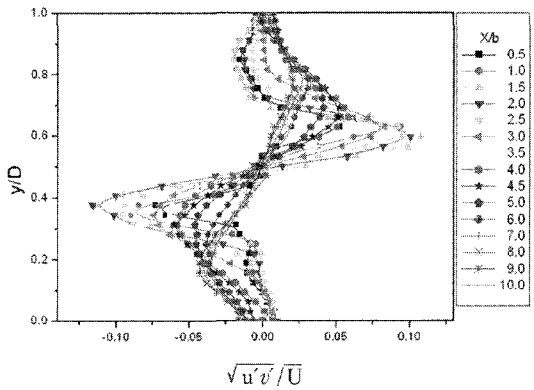

Fig. 31 Time-mean local Reynolds stress profiles without swirl behind the square cylinder for Re=30,000

without swirl behind the round cylinder. Even though it shows a bimodal profile like the turbulent intensity, the profile with swirl in Fig. 34 has the maximum value of y/D=0.9~1.0 near the tube wall and an asymmetric profile similar to the turbulent intensity. It is thought that this phenomenon is also caused by the tangential velocity of the swirl flow near the tube wall.

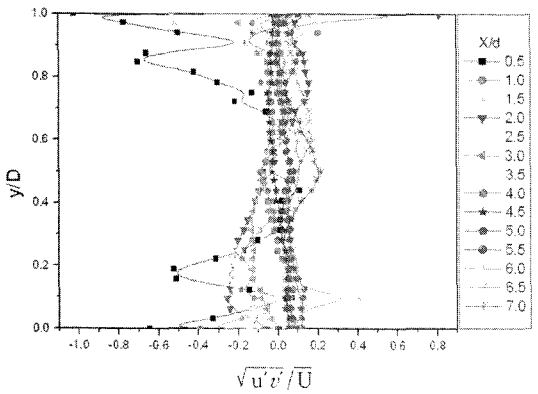

Fig. 32 Local Reynolds shear stress profile with swirl for Re=20,000 behind the round cylinder

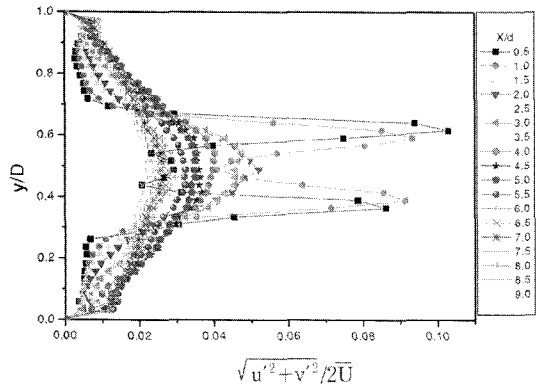

Fig. 33 Local kinetic energy profile without swirl for Re=30,000 behind the round cylinder

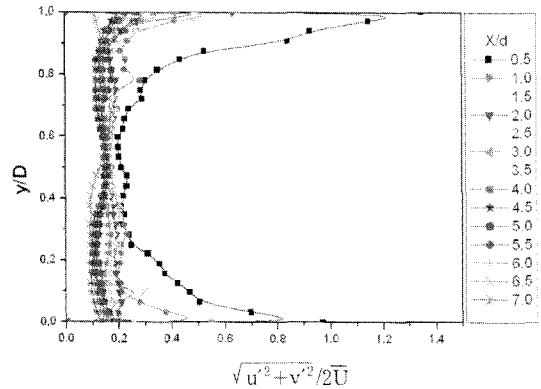

Fig. 34 Local kinetic energy profile with swirl for Re=20,000 behind the round cylinder

4. Conclusions

The following conclusion is obtained for the wake with and without swirl flow behind the round cylinder by PIV method.

(1) The axial velocity profiles with swirl have a re-circulating region at the entry of the round cylinder, and the more X/d is increased the shorter the region is. It is thought that this phenomenon is caused by the rotating direction of the tangential velocity in the swirl flow.

(2) In the centerline of the flow, $U/\overline{U}$ of the wake with swirl was 0.2~0.86 greater than that without swirl and in case without swirl, 0.0~−0.4 lower than that of swirl, but as the swirl was decayed after X/d=3.0, $U/\overline{U}$ of the wake with swirl had the same profile as that without swirl flow did.

(3) Axial turbulent intensity profile with swirl for Re=20,000 behind the round cylinder is shown the minimum value at y/D=0.2~0.9 near the tube wall and the maximum value at X/d=0~1.0 and y/D=0, 1.0 near the tube wall.

(4) The contour of the radial turbulent intensity profiles with swirl behind a cylinder. The profiles reach the minimum value at y/D=0.2~0.8 but the maximum near the test the tube wall. The swirl flow does not much affect the radial velocity component.

(5) The local Reynolds shear stress profile with swirl for behind the round cylinder shows negative shear stresses near the tube wall and asymmetric phenomena appears at y/D=0, 0.2 and y/D=0.8~1.0, but as the swirl is decayed, it approaches to 0 after X/d=3.0 and y/D=0.3~0.6.

(6) The kinetic energy profiles with swirl has the maximum value of y/D=0.9~1.0 near the tube wall and an asymmetric profile similar to the turbulent intensity. It is thought that this

phenomenon is also caused by the tangential velocity of the swirl flow near the tube wall.

Acknowledgments

This work was supported by Kyungnam University research fund, 2005.

References

Boo Jung-sook, 1985, "2 Dimensional Turbulent Structure Behind A Round Cylinder," *Ph. D Paper*, Kyungbuk University.

Cantwell, B. J., 1975, "A Flying Hot Wire Study of the Turbulent Near Wall of Circular Cylinder at a Reynolds Number of 140,000," California Institute of Technology.

Chew, Y. T., 2001, "Numerical Flow Visualization of Flow Over a Square Cylinder at Incidence," *Proceeding of the 6th Asian Symposium on Visualization*, pp. 70~72.

Cho, J. H., 1990, "A Study on Tubulent Flow Charateristics in the Wake of the Square Cylinder," *Chungnam University*, Master paper.

Choi, J. H. and Lee, S. J., 1999, "Effect of External Acoustic Excitation on Wake behind a Circular Cylinder," *KSME B*, Vol. 23-5, pp. 603~609.

Coles, D., 1983, "Prospects of Useful Research on Coherent Structure in Turbulent Shear Flow," *Proc. Indian Acad. Sci.*, (Engineering Sci.) 4: pp. 111~127.

Contanceau, M. and Bouard, R., 1959, "Experimental Determination of the Main feature of the Viscous Flow in the Wake of a Circular Cylinder in Uniform Translation," *Fluid Mechanics*, Vol. 79, No. 2, pp. 231~259.

Daichin and Sang Joon Lee, 2001, "Flow Field Analysis of Wake behind an Elliptic Cylinder Close to a Free Surface," *Proceeding of the 6th Asian Symposium on Visualization*, pp. 216~218.

Doh, D. H., 2001, "Probind 3-D Structures of the Wake Near a Circular Cylinder," *Proceeding of the 6th Asian Symposium on Visualization*, pp. 335~340.

Jang, D. S., Lee, Y. W., Doh, D. H., Kang, C. S. and Kobayashi, T., 2001, "Large Eddy of Flow around a Bluff Body of Vehicle shape," *Proceeding of the 6th Asian Symposiumon Visualization*, pp. 335~340.

Kim, K. C. and Jung, Y. B., 1995, "A Study on the Characteristics of Cylinder Wake Placed in Thermally Stratified Flow (IV) - On the Cylinder Wake with Various Heating Rates," *KSME*, Vol. 19-5, pp. 1340~1350.

Kiya, M. and Matsumura, M., 1985, "Turbulent Structure in Intermediate Wake of a Circular Cylinder," *JSME*, pp. 451~463.

Lee Hyun, 2001, "A Study on Fluid Characteristics in the Wake of Bluff Bodies by Multivision PIV," Korea Marine University Msc Theses.

Lee, M. B. and Kim, K. C. 2001, "A Study on the Near Wake of a Square Cylinder Using Particle Image Velocimetry (I)," *KSME B*, Vol. 25, pp. 1408~1416.

Mizota, T. and Okajima, A., 1981, "A Experimental Studies of Mean Flow around Rectangular Prisms," *Japan, Soc. Civ. Engrs 312*, pp. 39~47.

Okajima, A., 1982, "Strouhal Numbers of Rectangular Cylinders," *Kyushu Univ.*, pp. 379~398.

Owen, F. K. and Johnson, D. A., 1980, "Measurements of Unsteady Vortex Flow Fields," *AIAA*, Vol. 18, pp. 1173~1179.

Roshko, A., 1961, "Experimentals on the Flow Past a Circular Cylinder at Very High Reynolds Number," *J. of Fluid Mech.*, 10, pp. 345~356.

Tae-Hyun Chang and Jong-Boong Lee, 2004, "An Experimental Study on the Wake of a Square Cylinder Using Particle Image Velocimetry," *Journal of the Korean Society of Marine Engineers*, Vol. 24, No. 1, pp. 124~135.

Yoon, S. H., Sim, J. K., Woo, C. S. and Lee, D. H., 1999, "Influence of the Wake Behind Rectangular Bars on the Flow and Heat Transfer in the Linear Turbine Cascade," *KSME B*, Vol. 23-7, pp. 864~870.